International Journal of Engineering and Applied Sciences (IJEAS)
ISSN: 2394-3661, Volume-3, Issue-4, April 2016

Modelling of Permanent Magnets Track in the Finite Element Analysis of Linear Synchronous Motor

Petar Milkov Uzunov

***Abstract*—The paper presents a special technique for magnetic way modeling in its FEM - based (Finite Elements Method) analysis of the AC magnetic field, which aims at accurate calculation of forces acting on the moving part of one Permanent Magnet Linear Synchronous Motor (PMLSM). Here has been used an approximation of AC solutions of problems for linear motors with replacing the permanent magnet ways by AC current sheets. This models the synchronous movement of the magnets interacting with the AC currents in the mover winding. Calculated thrust and attractive force of the linear motor on the base of AC and DC motor magnetic field analysis was compared with the results from experiment and their good match has been proved.**

***Index Terms*—Permanent Magnet Linear Synhronous Motor, Finite Element Analysis, Permanent Magnet Ways, Modeling, Forces Calculation.**

I. Introduction

Today in competitive industrial environment linear motors can directly translate linear motion to machine tools without indirect coupling mechanisms such as gear boxes, chains and screws. In particular, permanent magnet direct drive linear motors are becoming more and more popular in machine automation nowadays. The advantages of permanent magnet motor drives are their gearless structure, excellent control characteristics such as high speed, high acceleration and most importantly, high motion precision and better efficiency. PMLSM are used in lifts [1], linear transportation systems[1]-[3], industrial laser systems *etc*.

In PMLSM, the moving part (mover) consists of a slotted armature and three-phase windings, while the surface permanent magnets are mounted along the whole length of the path (stator) and are arranged in magnetic ways (MAW).

Modern PMLSM consist of three types of materials: ferromagnetic material, electrical conductor material and electrical insulator material. The ferromagnetic materials include the permanent magnets (PM) and iron. Electrical motors use mainly rare-earth PM. These materials are characterized by a large hysteresis cycle and have a high coercive magnetic field *Hc*. MAW produce the excitation flux

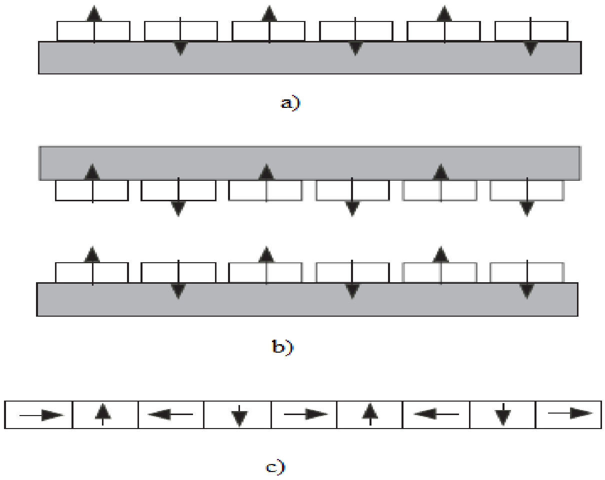

Fig. 1. Different types of magnetic ways: a) surface mounted PM; b) double sided magnetic ways; c) Halbach array [1]

in the air gap. Magnets, which are the magnetic source, can be either mounted or inserted in a magnetic yoke or combined to form an Halbach array [1]. These three families of MAW are presented on Fig. 1. The first group consists of magnets mounted on a yoke surface (Fig. 1a). Furthermore, double sided MAWs (Fig. 1b) are used with a supply part without iron. These types of motors are sometimes called "ironless" motors [1], [2].

Halbach array (Fig.1c) have a particularity due to the magnet placing, since they have a magnetic flux enhanced on one side (strong side) and cancelled on the other side (weak side).

All magnetic ways are presented in a short stator configuration i.e. the MAW are fixed.

Modeling of PM is a special topic when FEM is used for solving of the linear motors magnetic field and this paper presents a unique method for this purpose, regarding the capabilities of used software - FEMM [4].

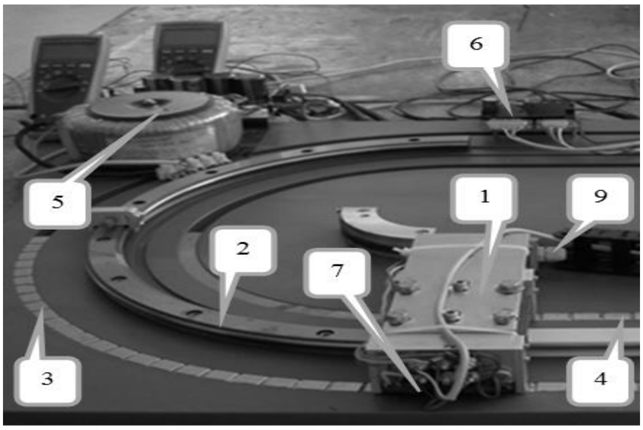

a)

Peter Milkov Uzunov, Electricity System Operator, Sofia, Bulgaria, +35966876342/ +359878740323

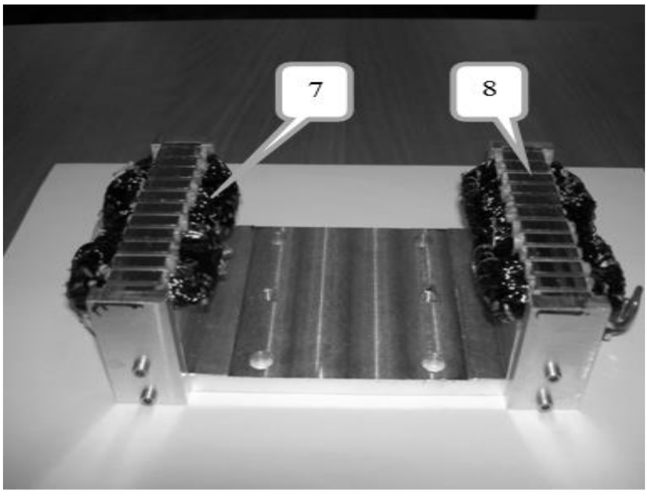

b)

Fig. 2. Servomotor PMLSM-1 prototype: a) PMLSM-1; b) movable part of the motor: 1-motor; 2- linear guidance ; 3,4- MAWs; 5- DC supply source; 6- digital servo drive; 7- windings; 8- ferromagnetic cores; 9- head of magnetic encoder

The object of modeling in this work is the first designed and manufactured in Bulgaria prototype of PMLSM-1 shown in Fig. 2a [5].The linear motor has the original "two-legged frame" of the mover, shown in Fig. 2b, to obtain a balance of the mechanical system according the attraction forces. On each of the two magnetic cores was wound three-phase distributed winding (Fig. 2b). Each coil is "star" connected and the two coils are connected in series. The main specifications of studies of linear motor are arranged in Table I.

TABLE I
SPECIFICATIONS OF THE TEST BENCH

N	Quantity	Value
1	Number of phases	3
2	Number of poles	4
3	Slot number	12
4	Rated phase voltage [V]	70
5	Rated phase current [A]	6
6	Rated thrust [A]	140
7	Rated speed [m/s]	3
8	Air gap [mm]	1

II. FEM MODELING

A. Field equations

The motor magnetic field modeling is based on the Maxwell's laws together with their simplifications. Here was modeled the stationary magnetic field in 2D case. The important contribution in the field of magnetism done by J.C. Maxwell was to regroup a set of equations which allows to join together the electrostatic and electromagnetic theories. These equations, reduced thereafter to four by means of the vector calculation, are presented in differential form.

The general differential form of the Maxwell's equations is [6]:

$$\vec{\nabla} \times \vec{H} = \vec{J} + \frac{\partial \vec{D}}{\partial t} + \rho_c \vec{v}\,; \tag{1}$$

$$\vec{\nabla}\, \vec{D} = \rho_c\,; \tag{2}$$

$$\nabla \times \vec{E} = \frac{\partial \vec{D}}{\partial t}\,; \tag{3}$$

$$\vec{\nabla}\, \vec{B} = 0\,. \tag{4}$$

where

$\vec{E}$ is the vector of electric field;
$\vec{D}$ is the vector of electric displacement;
$\vec{H}$ is the vector of magnetic field strength;
$\vec{B}$ is the vector of magnetic flux density;
$\vec{J}$ is a vector of current density;
$\vec{v}$ the linear velocity ;
ρ_c is the volume charge density.

In motor modelling only quasi-static electromagnetic problems are studied and the time-derivate of current displacement can be neglected compared to the current density. Therefore, (1) can be simplified to:

$$\vec{\nabla} \times \vec{H} = \vec{J}\,, \tag{5}$$

implying:

$$\vec{\nabla}\, \vec{J} = 0\,. \tag{6}$$

Furthermore, the study of electric field in dielectric material is not the main point of interest here which is why (2) is not used in this study.

In addition to this set of equations, the properties of materials have to be introduced by set of constitutive equations. The first equation puts in relation the magnetic flux density $\vec{B}$ and the magnetic field $\vec{H}$ in a material:

$$\vec{B} = \mu \vec{H}\,. \tag{7}$$

Here, μ is the permeability of the materials.

The second constitutive equation puts in relation the current density and the electric field in a conducting medium of conductivity γ:

$$\vec{J} = \gamma \vec{E}\,. \tag{8}$$

This equation is known as the generalized Ohm's law and it allows to determine electrical resistance.

Furthermore, from (4) by applying one property of vector calculation (the divergence of the rotational of a vector is null) a magnetic potential vector $\vec{A}$ is defined as:

$$\vec{B} = rot\,\vec{A}\,. \tag{9}$$

If a material is nonlinear (*e.g.* saturated iron or NdFeB magnets), the permeability, μ is actually a function of $\vec{B}$:

$$\mu = \frac{\vec{B}}{\vec{H}(\vec{B})}\,. \tag{10}$$

Now, this definition of *B* always satisfies (4). Then (5) can be rewritten as:

$$\vec{\nabla} \times \left(\frac{1}{\mu(\vec{B})} \vec{\nabla} \times \vec{A} \right) = \vec{J}\ . \tag{11}$$

For a linear isotropic material (and assuming the Coulomb gauge, $\vec{\nabla}\ \vec{A} = 0$), and (11) reduces to:

$$-\frac{1}{\mu} \vec{\nabla}^2 \vec{A} = \vec{J}\ . \tag{12}$$

In the general 3-D case, $\vec{A}$ is a vector with three components. However, in the 2-D planar and axisymmetric cases, two of these three components are zero, leaving just the component in the "out of the page" direction.

The advantage of using the vector potential formulation is that all the conditions to be satisfied have been combined into a single equation. If $\vec{A}$ is found, $\vec{B}$ and $\vec{H}$ can then be deduced by way of differentiating $\vec{A}$. The form of (11), an elliptic partial differential equation, arises in the study of many different types of engineering phenomena. There are a large number of tools that have been developed over the years to solve this particular problem [4].

Distribution of linear motor static magnetic field can be found by solving the equation (11) with the FEMM software . This software retains the form of (11), so that magneto-static problems with a nonlinear *B-H* relationship can be solved.

The problem was solved in area, shown on Fig. 3.

B. *Material properties*

The electrical and magnetic properties of materials for each part of the presented model were assigned (Fig. 3). Their properties are given in Table III.

A notable advantage of the FEA of electrical machines magnetic field using FEMM program is the ability to solve

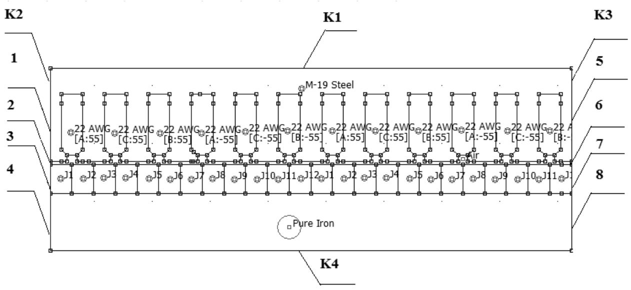

Fig. 3. FEMM model of linear synchronous servomotor

TABLE IIII
MAGNETIC AND ELECTRIC PROPERTIES OF USED MATERIALS

N	Model area	Material	Property	
			Conductivity (10^6 S/m)	Permeability (H/m)
1	Back iron	Steel 1018	5.8	BH curve 1
2	Air gap	Air	0.0	1
3	Permanent magnet	NdFeB grade N37	0.67	BH curve 2
4	Winding	Copper wire IIET-2F, Diam. 0.65 mm	58	1
5	Mover core	Silicon steel 2212, Thicknes 0.5 mm	1.96	BH curve 3

nonlinear tasks i.e. consider the strong non-linearity of characteristics of magnetic materials used. This is done by means of so-called "BH curves" [4] representing dependencies $B = f\,(H)$ for the corresponding material. On Fig. 4a, 4b, and 4c are shown the curves for the materials in Table III.

A. *MAW Modeling*

Magnets can be modeled from several different, but equally valid, points of view [2],[4],[7]. Concerning finite elements analysis the most useful model is to regard the magnet as a volume of ferromagnetic material surrounded by a thin sheet of current [4].

During AC simulation of PMLSM by means of FEMM software there arises a serious *problem* : it seems impossible

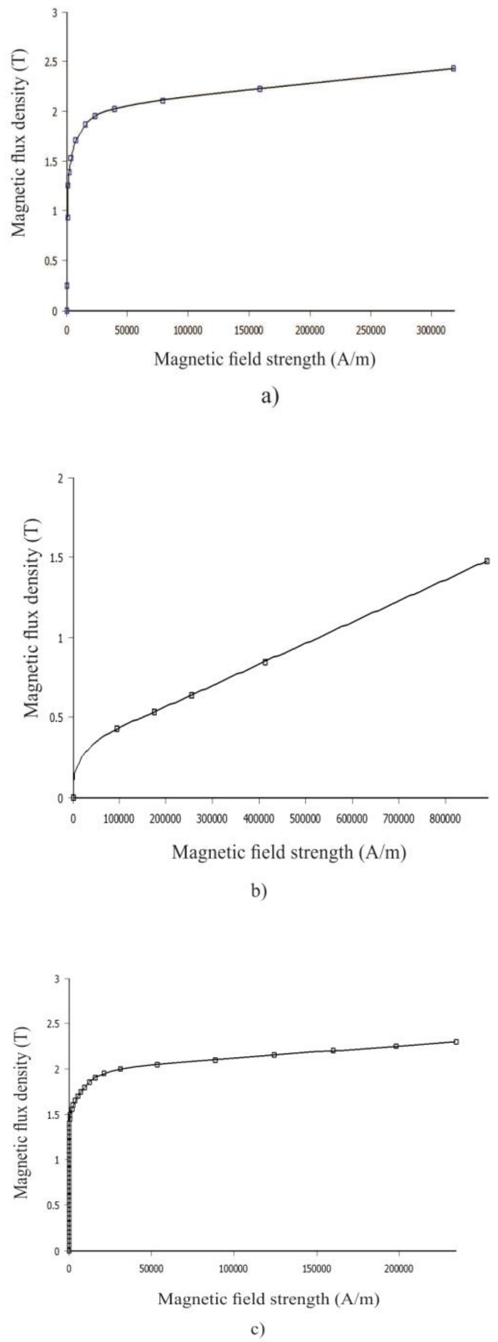

Fig. 4. Initial curves of magnetization: a) BH curve 1; b) BH curve 2; c) BH curve 3

to solve the task of the FEA of the stationary magnetic field produced by permanent magnets and the quasi-stationary field produced by AC in the three-phase motor winding.

AC problems in FEMM consider excitation at only one frequency f at a time i.e. FEMM *only works with a single frequency at a time*! The User cannot mix DC magnetic field excited PMs with AC magnetic field from the windings. This means that PMs ($f = 0$ Hz) and electromagnets – windings with AC current in them ($f > 0$ Hz) cannot be simulated together. It indicates that the user cannot draw the magnets and the coils and set a current frequency and get the corresponding force (or torque) – FEMM will ignore the permanent magnet's fields and give us the torque that resulted only from the AC-induced field [4].

A *second problem*: In simulation process one really wants to move the PMs and back iron of the linear motor synchronously with the currents to get meaningful results, however, in FEMM software all AC solutions have a constant physical configuration [4].

For solving this problem there is a way to approximate AC solutions for brushless motors' problems by replacing the magnets with AC current sheets. This models the synchronous movement of the magnets interacting with the AC currents in the stator. It is good for computing stator core losses, for example and also yields force estimates that are consistent with the DC results.

In the study presented such approach was used for modeling of sinusoidal wave of PMs magnetic field. The magnetic field produced by PMs of alternating polarity is modeled using the equivalent currents densities. They create a magnetic field with sinusoidal distribution along the track of PMs.

To practically implement this approach it is advisable to proceed as follows:

- The length of the magnetic way of modeled linear motor is equal to four times the pole pitch. It is divided into twelve equal sections. For each of them is set a linear magnetic material with a relative permeability equal to that of the permanent magnets
-

$$\mu_r = \frac{B_r}{\mu_0 H_c} . \tag{13}$$

- for each of these sections is set current density, according to the equation
-

$$j_k = \frac{4H_c}{\tau} e^{j\frac{k\pi}{6}} , \tag{14}$$

where $k = 0,1,2,3...11$.

In this way there is modeled the sinusoidal distribution of the field created by the PMs .

B. Modeling of motor winding

For the complete formulation of the task there should be modeled a three-phase winding of the mover. The distribution of the individual slots in the three phases is shown in Fig. 5.

In Fig .5 the part of the area corresponding to the slots of the mover core and the amplitudes of three-phase current system was set according equations

$$\begin{aligned} \dot{I}_{Am} &= I_m e^{j0} ; \\ \dot{I}_{Bm} &= I_m e^{j\frac{2\pi}{3}} ; \\ \dot{I}_{Cm} &= I_m e^{-j\frac{2\pi}{3}} , \end{aligned} \tag{15}$$

where I_m is the motor current amplitude and angular frequency is

$$\omega = 2\pi f . \tag{16}$$

In (16) frequency can be calculated as follows

$$f = \frac{v}{2\tau_p} , \tag{17}$$

where

v is the motor linear speed;

τ_p – pole pitch.

In Fig. 6. is shown the distribution of real and imaginary part of the normal component of magnetic flux density in the air along the MAW model over the distance of 0.5 mm from the upper MAW surface i.e in the air gap of the linear motor

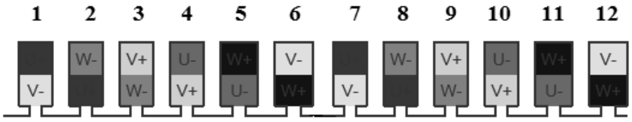

Fig. 5. Double layer full pitch winding layout 2p=4 poles and z = 12 slots

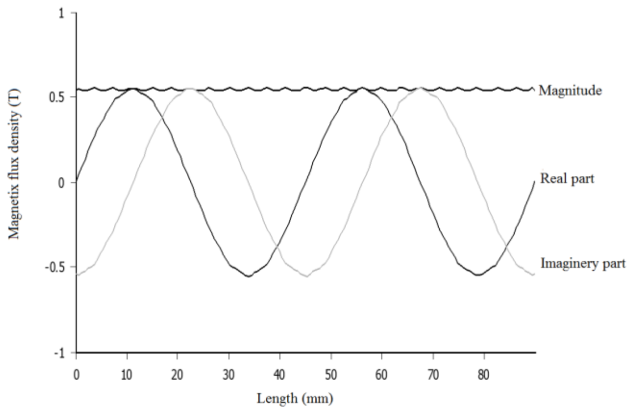

Fig. 6. Distribution of the real and imaginary part of magnetic field density near the MAW model surface.

without mover. In this case the magnetic field was excited only by the current densities that were used for MAW modeling. It is seen that distribution is sinusoidal with magnitude of magnetix flux density 0.55 T.

C. Boundary conditions

In the model Periodic boundary conditions [4] were used. They allow to model the linear motor as rotational one. As is known from the theory of PMLSM, these may be obtained if cut to the axis of a rotational synchronous motor with PMs and expanded in one plane. In order to implement the periodic boundary conditions practically vertical boundary contours K2 and K3 (Fig. 3) must be of absolutely identical structure i.e. types of lines (1 ÷ 8) and their lengths must be equal as well.

On the other two boundaries K1 and K4 are set Dirichlet boundary conditions for the magnetic vector potential, according to the equation

$$\vec{A}\Big|_{K1,K4} = 0. \tag{18}$$

The problem domain was discretized on the FEM mesh with 32648 nodes and 64891 triangular finite elements.

D. FEA results

As a result of FEA of the quasi-stationary linear motor magnetic field by solving equation (12) are obtained the values of the magnetic vector potential $\vec{A}$. The magnetic flux density $\vec{B}$ and intensity of the magnetic field $\vec{H}$ in each node of the solution area was deduced by differentiating the magnetic vector potential $\vec{A}$. The distribution of the magnetic flux density for the modeled linear motor is shown in Fig. 7.

The four poles of motor magnetic field was clearly shown on Fig. 7.

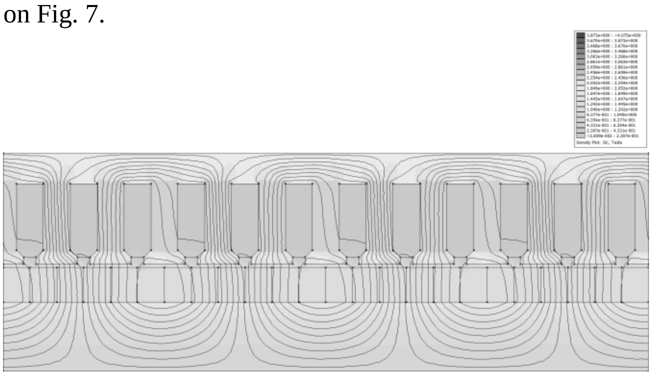

Fig. 7. Magnetic flux distribution from AC simulation

E. Force calculations

The forces acting on the motor mover - thrust and force of attraction between mover core and PMs can be calculated based on the FEM magnetic field analysis results via Weighted Stress Tensor integral [4].

This volume integral greatly simplifies the computation of forces and torques. Merely select the blocks or conductors upon which force or torque are to be computed and evaluate the integral. Nothing special is required in getting good force results (as opposed to the Stress tensor line integral), although results tend to be more accurate with finer meshing around the region upon which the force is to be computed [4].

The results from forces calculation are shown in Table IV

III. FEA OF PMLSM STATIONARY MAGNETIC FIELD EXCITED BY THE DC CURRENT IN WINDINGS

Verification of the method for MAW modeling of the motor magnetic field can be made in two ways: indirectly by comparing thrust and force of attraction between mover and PMs calculated with FEA during modeling of PMs with the same forces, but calculated on the grounds of magnetic field analysis results. Said magnetic field is excited by direct currents in motor winding whose magnitudes are equal to the rms values of real phase currents passing through the winding.

The second way employs direct comparison of calculated forces taken into account during modeling and the results from their measuring during investigation of the linear motor prototype PMLSM-1.

For the analysis of linear motor magnetic field excited via DC current in motor winding and PMs in MAW new FEM model of the motor must be built. With this model PMs are included with their real sizes and properties as shown in Fig. 8.

The phases of the mover winding were supplied with DC currents whose values are equal to those of the instantaneous motor currents, calculated as follows:

TABLE IIIV
THRUST AND FORCE OF ATTRACTION FROM FEM CALCULATION

Forces [N]	FEM calculation
Thrust F_x	119.56
Force of attraction F_y	897.12

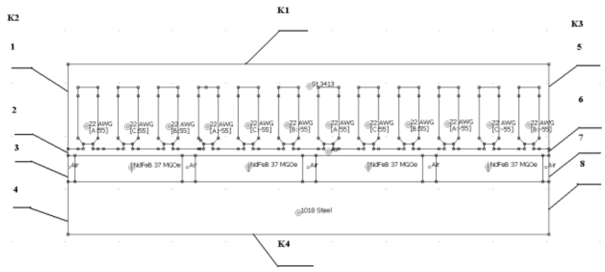

Fig. 8. The FEMM model of PMLSM with PMs

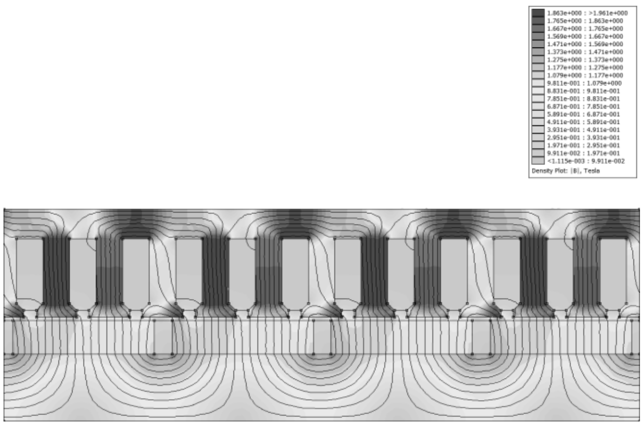

Fig. 9. DC magnetic flux distribution

$$\begin{aligned} i_A &= I_m \cos\omega t; \\ i_B &= I_m \cos(\omega t - \frac{2\pi}{3}); \\ i_C &= I_m \cos(\omega t - \frac{4\pi}{3}). \end{aligned} \tag{19}$$

Moreover, according to the first law of Kirchhoff the sum of the currents in all three phases must be zero, because the motor winding is "star" connected. Motor materials and boundary conditions remain the same as before. The distribution of the magnetic flux density in the solved area is received by solving (12) and differentiation of the magnetic vector potential. This distribution can be seen on Fig. 9.

The results from the new calculations of forces are given in Table V.

As can be seen from Table V calculated force values are very close to these in Table IV. This is a good verification of method described in the previous paragraph for MAW modeling in linear motor AC FEA.

IV. Experimental Validation of the Results from Force Calculations

To verify the simulations results and the calculation results of linear motor thrust and force of attraction an experimental setup, shown in Fig. 10, was used.

The prototype of PMLSM-1 is controlled by the digital servo controller 2 [8], which is connected via interface and the USB connector to the computer. The direct current source 3 supplies the digital controller at two voltages: 12V for control circuits and 140V for power circuits. Consumed DC current and voltage from digital controller are measured by digital multimeters 4 and 5. The motor line to line voltage and current are measured directly from the digital controller which displays them by GDTool software [9].

TABLE V
THRUST AND FORCE OF ATTRACTION FROM FEM CALCULATION

Forces [N]	FEM calculation
Thrust F_x	130.26
Force of attraction F_y	978.48

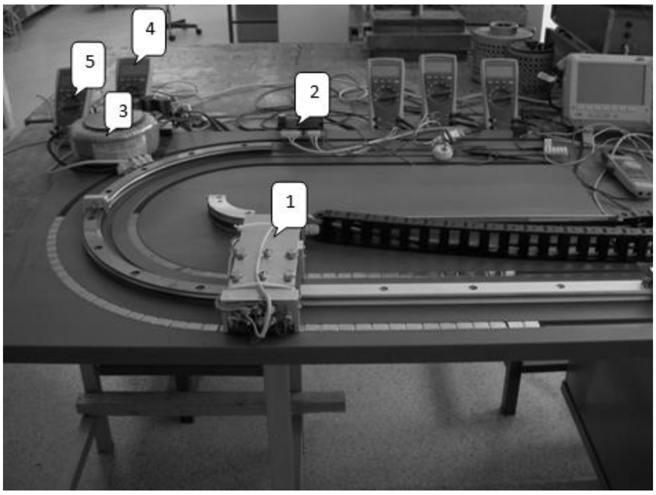

Fig. 10. Experimental setup for PMLSM-1

Because the mover position *x* versus time *t* is known from the servo drive software, the mover speed v and acceleration *a* can be calculated by numerical differentiation

$$v = \frac{dx}{dt}; \tag{20}$$

$$a = \frac{dv}{dt}. \tag{21}$$

Calculation of the linear motor thrust can be made by the following equation:

$$F_{thrust} = ma, \tag{22}$$

where *m* is the mass of the mover without the payload.

The attraction force F_{attr} can be estimated with similar mechanical experiment in no-load mode and without currents in motor windings.

This force is equal to the force F_y that must be applied to detach the movable part of the motor from the permanent magnet attraction provided when 1 mm thick pad of non-magnetic material was inserted to fill the gap between these two motor parts .

TABLE VI

COMPARISION OF EXPERIMENTAL AND FEM CALCULATIONS

Motor parameters	AS simulation	DC simulation	Experiment
Thrust F_x (N)	119,56	130,26	140,6
Relative error ε_1 (%)	-15	-7,3	-
Force of attraction F_{attr} (N)	897.12	978.48	950
Relative error ε_2 (%)	-5.6	3	-

The experimental cinematic diagram for attraction force estimation is shown in Fig. 11.

Experimental results are compared in Table VI with those from the simulations carried out by FEM.

V. Conclusion

The study presented in here makes use of a unique approach for modeling on the MAW of one linear synchronous servo motor in the FEM analysis of its quasi-stationary magnetic field excited by AC in the winding. In this approach magnetic field produced by MAWs PMs with alternating polarity was modeled using the equivalent current densities. They create a magnetic field with a sinusoidal distribution along the track of PMs.

Verification of the proposed method is made indirectly by calculating the forces, acting on the mover – thrust and force of attraction of the mover to the PMs, based on the results of the analysis of the linear motor magnetic field with FEM. First, these two forces are compared with the values calculated on the basis of the analysis of the stationary

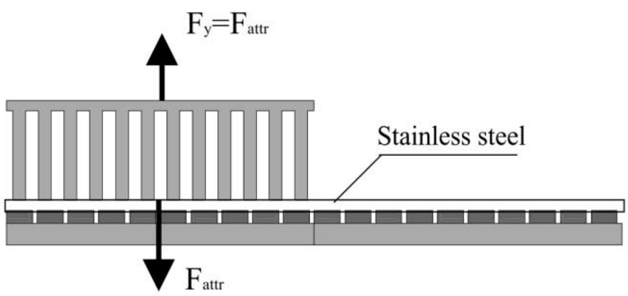

Fig. 11. Experimental setup for attraction force measurement

magnetic field excited by the DC currents in the motor winding for the same position of the mover to PMs.

Secondly, the values of these two forces are compared with the measured values during experimental study of the linear motor prototype PMLSM-1.

It has been found that in the case of the DC simulation results of force calculation are better and very close to the experimental ones. For this reason during the design of the PMLSM it is more appropriate to calculate the thrust and force of attraction based on the results of the FEM analysis of the stationary magnetic field of the linear motor.

ACKNOWLEDGMENT

The author expresses his gratitude to Dr. David Meeker for his assistance, support and contribution to the application of his program FEMM in the process of simulations and to Prof. Jacek F. Gieras for his support in the design process of the linear motor.

REFERENCES

[1] J. F. Gieras, Zbigniew J. Piech, *Linear Synchronous Motors: Transportation and Automation Systems*, Taylor & Francis, 1999.
[2] S. Chevailler, "Comparative study and selection criteria of linear motors", Ph.D. Thesis, EPFL, Suisse, 2006, pp.3-9.
[3] Beckhoff New Automation Technology, "XTS. eXtended Transport System", Corporative brochure, 2012, [Online]. Available: www.beckhoff.com
[4] D. Meeker, (2015, Oct). FEMM reference manual. [Online]. Available: http://www.femm.info/Archives/doc/manual42.pdf
[5] P. M. Uzunov "Linear electromagnetic transportation system," Mechatronica SC, Gabrovo, Bulgaria, Tech. Rep. on Contract NIF-02-22 / 15.12.2012 / Executive Agency for Promotion of Small and Medium-sized Enterprises, 2015.
[6] Bo Thide, *Electromagnetic field theory*, Upsiln Books, Uppsala, Sweden, 1997, pp. 1-14.
[7] P.M. Uzunov, S. Jordanov, Modeling of permanent magnets in the analysis of electromagnetic devices with the Finite Element Method, Journal of the Technical University of Gabrovo, Vol. 36, 2008, pp. 75-78.
[8] T. Kotkanen, Granite Device Knowledge Wiki, [Online].Available: http://granitedevices.com/wiki/VSD-E_and_VSD-XE
[9] T. Kotkanen, (2015). GDtool. [Online]. Available http://granitedevices.com/wiki/GDtool

Petar M. Uzunov was born in 1962 in the town of Suhindol, region of Veliko Tarnovo , Bulgaria. He took his B.Sc. and M.Sc. degrees in Electrical Engineering from the Technical University of Gabrovo, Bulgaria in 1988 and Ph.D. degree in Electrical Engineering from the same University in 1998.

From 1988 to 2007, he held teaching positions as Assistant Professor, Senior Assistant Professor, Chief Assistant Professor and Associate Professor at the " Fundamentals of Electrical and Power Engineering Department at Technical University of Gabrovo. From 2008 to 2012, he has chaired the same Department. From 2012 to 2015 he has headed R&D Department at Mechatronica SC in Gabrovo, Bulgaria. Currently he is with Electricity System Operator, Sofia, Bulgaria. From 2010 to 2012 he was a member of IEEE. Assoc. Prof. Petar Uzunov, Ph.D authored 10 textbooks, more than 65 articles, and two inventions. His research interests include optimal design of electrical machinery, simulations and research of electromagnetic processes in electrical machines and apparatus based on the analysis of electromagnetic field through Finite Element Method and hysteresis modeling.